Supporting Information

A Facile Radiolabeling of [^{18}F]FDPA via Spirocyclic Iodonium Ylides: Preliminary PET Imaging Studies in Preclinical Models of Neuroinflammation

Lu Wang,[†,§] Ran Cheng,[†,¶,§] Masayuki Fujinaga,[‡,§] Jian Yang,[#] Yiding Zhang,[‡] Akiko Hatori,[‡] Katsushi Kumata,[‡] Jing Yang,[#] Neil Vasdev,[†] Yunfei Du,[¶] Chongzhao Ran,[#] Ming-Rong Zhang[*,‡] and Steven H. Liang[*,†]

[†] Division of Nuclear Medicine and Molecular Imaging, Massachusetts General Hospital & Department of Radiology, Harvard Medical School, Boston, MA, 02114, USA.

[‡] Department of Radiopharmaceutics Development, National Institute of Radiological Sciences, National Institutes for Quantum and Radiological Science and Technology, 4-9-1 Anagawa, Inage-ku, Chiba 263-8555, Japan.

[¶] School of Pharmaceutical Science and Technology, Tianjin University, Tianjin, 300072, China.

[#] Athinoula A. Martinos Center for Biomedical Imaging, Massachusetts General Hospital & Department of Radiology, Harvard Medical School, Charlestown, MA, 02129, United States.

[§] These authors contribute equally to this work.

Contents

1. General considerations

All the chemicals employed in the syntheses were purchased from commercial vendors and used without further purification. Thin-layer chromatography (TLC) was conducted with 0.25 mm silica gel plates (^{60}F-254) and visualized by exposure to UV light (254 nm) or stained with potassium permanganate. Flash column chromatography was performed using silica gel (particle size 0.040-0.063 mm). H-Nuclear magnetic resonance (NMR) spectra were obtained at 300 MHz on Bruker spectrometers in $CDCl_3$ or d_6-DMSO solutions at room temperature with tetramethylsilane (TMS, δ = 0) as an internal standard. ^{13}C NMR spectra were obtained at 75 MHz. Chemical shifts (δ) are reported in ppm and coupling constants are reported in Hertz. The multiplicities are abbreviated as follows: s = singlet, d = doublet, t = triplet, m = multiplet, br = broad signal, dd = doublet of doublets, etc. For all the HRMS measurements, the ionization method is ESI and the mass analyzer type is TOF. Radiochemical incorporation yields (RCCs) were determined by radioTLC. EMD TLC Silica gel 60 plates (10 x 2 cm) were spotted with an aliquot (1-5 μL) of crude reaction mixture approximately 1.5 cm from the bottom of the plate (baseline). TLC plates were developed in a chamber containing ethyl acetate and methanol (EtOAc/MeOH = 8:1) until within 2 cm of the top of the plate (front). Analysis was performed using a Bioscan AR-2000 radio-TLC imaging scanner and WinScan software. Radiochemical identity and purity were determined by radioHPLC. A Phenomenex Luna C18, 250 x 4.6 mm, 5 μm HPLC column was used with a Waters 1515 Isocratic HPLC Pump equipped with a Waters 2487 Dual λ Absorbance Detector, a Bioscan Flow-Count equipped with a NaI crystal, and Breeze software. Each radiochemical labeling was conducted at least three times ($n \geq 3$).

2. **Chemistry**

3-cyano-*N,N*-diethyl-4-(4-fluorophenyl)-4-oxobutanamide (6). To a solution of 3-(4-fluorophenyl)-3-oxopropanenitrile **3** (400 mg, 2.45 mmol) and 2-chloro-*N,N*-diethylacetamide **5** (342 mg, 2.28 mmol) in 80% EtOH (16 mL) were added NaOH (88 mg, 2.28 mmol) and NaI (1.03 g, 6.84 mmol). The mixture was irradiated in a Biotage Initiator at 80 °C for 40 min, then was filtered and extracted with CH_2Cl_2. The residue was concentrated and purified with flash chromatography on silica gel (Hexane/EtOAc = 1/1, v/v) to afford **6** (346 mg, 1.25 mmol, 55%) as a yellow oil. ^{1}H NMR (300 MHz, $CDCl_3$) δ 8.08 (dd, *J* = 8.1, 5.1 Hz, 2H), 7.12 (t, *J* = 8.4 Hz, 2H), 4.97 (dd, *J* = 9.3, 4.2 Hz, 1H), 3.43-3.23 (m, 5H), 2.87 (dd, *J* = 16.2, 4.2 Hz, 1H), 1.24 (t, *J* = 7.2 Hz, 3H), 1.05 (t, *J* = 6.9 Hz, 3H). Characterization confirmed by comparison with published characterization data.[1]

3-cyano-*N,N*-diethyl-4-(4-iodophenyl)-4-oxobutanamide (7). Starting from 3-(4-iodophenyl)-3-oxopropanenitrile **4** (664 mg, 2.45 mmol), similar procedure was conducted to produce **7** (543 mg, 1.42 mmol, 62%) as a light yellow solid. ^{1}H NMR (300 MHz, $CDCl_3$) δ 7.90 (d, *J* = 8.7 Hz, 2H), 7.75 (d, *J* = 8.7 Hz, 2H), 4.95 (dd, *J* = 9.6, 4.2 Hz, 1H), 3.45-3.30 (m, 5H), 2.82 (dd, *J* = 16.2, 4.2 Hz, 1H), 1.27 (t, *J* = 6.9 Hz, 3H), 1.08 (t, *J* = 7.2 Hz, 3H). Characterization confirmed by comparison with published characterization data.[2]

2-(3-amino-5-(4-fluorophenyl)-1*H*-pyrazol-4-yl)-*N,N*-diethylacetamide (8). To a solution of **6** (553 mg, 2 mmol) in EtOH (10 mL), hydrazine hydrate (4 mmol, 0.19 mL) and acetic acid (0.2 mL) were added and the reaction mixture was heated at 80 °C for 8 h. After cooling, the mixture was concentrated and purified with flash chromatography on silica gel ($CHCl_3$/MeOH = 10:1, v/v) to afford **8** (511 mg, 1.76 mmol, 88%) as a white solid. ^{1}H NMR (300 MHz, $CDCl_3$) δ 7.37-7.42 (m, 2H), 7.11-7.19 (m, 2H), 6.08 (br s, 2H), 3.50 (s, 2H), 3.43 (q, *J* = 6.7 Hz, 2H), 3.12 (q, *J* = 7.5 Hz, 2H), 1.09 (t, *J* = 7.5 Hz, 3H), 0.96 (t, *J* = 6.7 Hz, 3H). Characterization confirmed by comparison with published characterization data.[1]

2-(3-amino-5-(4-iodophenyl)-1*H*-pyrazol-4-yl)-*N,N*-diethylacetamide (9). Starting from 3-cyano-*N,N*-diethyl-4-(4-iodophenyl)-4-oxobutanamide **7** (768.4 mg, 2 mmol), similar procedure was conducted to produce **9** (661 mg, 1.66 mmol, 83%) as a light yellow solid. ^{1}H NMR (300 MHz, $CDCl_3$) δ 7.77 (d, *J* = 8.1 Hz, 2H), 7.12 (d, *J* = 8.4 Hz, 2H), 3.49 (s, 2H), 3.34 (q, *J* = 6.9 Hz, 2H), 3.09 (q, *J* = 7.2 Hz, 2H), 1.09 (t, *J* = 7.2 Hz, 3H), 0.97 (t, *J* = 6.9 Hz, 3H). Characterization confirmed by comparison with published characterization data.[2]

***N,N*-diethyl-2-(2-(4-fluorophenyl)-5,7-dimethylpyrazolo[1,5-a]pyrimidin-3-yl)acetamide (10)**. To a solution of the 2-(3-amino-5-(4-fluorophenyl)-1*H*-pyrazol-4-yl)-*N,N*-diethylacetamide **8** (290.3

mg, 1 mmol) in EtOH (5 mL) the pentane-2,4-dione (100 mg, 1 mmol) was added and the mixture was heated at 80 ˚C for 4 h. The progress of reaction was monitored by TLC. After cooling, the mixture was concentrated and purified with flash chromatography on silica gel ($CHCl_3$/MeOH = 10:1, v/v) to afford **10** (266 mg, 0.75 mmol, 75%) as a white solid. Mp 137-139°C. ^{1}H NMR (300 MHz, $CDCl_3$) δ 7.85-7.80 (m, 2H), 7.11 (t, *J* = 8.6 Hz, 2H), 6.49 (s, 1H), 3.88 (s, 2H), 3.50 (q, *J* = 7.3 Hz, 2H), 3.38 (q, *J* = 7.2 Hz, 2H), 2.70 (s, 3H), 2.51 (s, 3H), 1.19 (t, *J* = 7.0 Hz, 3H), 1.09 (t, *J* = 7.2 Hz, 3H). Characterization confirmed by comparison with published characterization data.[1]

***N,N*-diethyl-2-(2-(4-iodophenyl)-5,7-dimethylpyrazolo[1,5-a]pyrimidin-3-yl)acetamide (11)**. Starting from 2-(3-amino-5-(4-iodophenyl)-1*H*-pyrazol-4-yl)-*N,N*-diethylacetamide **9** (398 mg, 1 mmol), similar procedure was conducted to produce **11** (370 mg, 0.8 mmol, 80%) as a white solid. ^{1}H NMR (300 MHz, $CDCl_3$) δ 7.78 (d, *J* = 6.6 Hz, 2H), 7.60 (d, *J* = 6.9 Hz, 2H), 6.53 (s, 1H), 3.91 (s, 2H), 3.54 (q, *J* = 7.2 Hz, 2H), 3.42 (q, *J* = 6.9 Hz, 2H), 2.74 (s, 3H), 2.54 (s, 3H), 1.23 (t, *J* = 7.2 Hz, 3H), 1.11 (t, *J* = 7.2 Hz, 3H). Characterization confirmed by comparison with published characterization data.[2]

2-(2-(4-((7,9-Dioxo-6,10-dioxaspiro[4.5]decan-8-ylide-ne)-λ^3-iodaneyl)phenyl)-5,7-dimethylpyrazolo[1,5*a*]pyrimidin-3-yl)-*N,N*-diethylacetamide (13). Starting from compound **11** (50 mg, 0.11 mmol), similar procedure (see experimental section in the manuscript) was conducted to produce the ylide precursor **13** (15 mg, yield over two steps 22%) as a white solid. Mp 137-139˚C. ^{1}H NMR (300 MHz, DMSO) δ 7.87-7.81 (m, 4H), 6.90 (s, 1H), 3.90 (s, 2H), 3.50 (q, *J* = 7.6 Hz, 2H), 3.30 (s, 3H), 3.24 (q, *J* = 7.7 Hz, 2H), 2.69 (s, 3H), 1.98 (d, *J* = 4.2 Hz, 4H), 1.69 (d, *J* = 6.7 Hz, 4H), 1.17 (t, *J* = 7.1 Hz, 3H), 0.97 (t, *J* = 6.9 Hz, 3H); ^{13}C NMR (75 MHz, DMSO) δ 169.2, 164.0, 158.4, 152.4, 147.6, 145.2, 136.4, 133.0, 130.5, 116.3, 112.6, 109.5, 102.2, 60.2, 59.1, 42.1, 37.3, 27.7, 24.7, 23.2, 21.2, 16.7, 14.7, 14.5, 13.5; HRMS (m/z): $[M+Na]^+$ calculated for 653.1237, found 653.1239.

2-(2-(4-(((1r,3r,5r,7r)-4',6'-Dioxospiro[adamantane-2,2'-[1,3]dioxan]-5'-ylidene)-λ3-iodane-yl)phenyl)-5,7-dimethy-lpyrazolo[1,5-a]pyramidin-3-yl)-N,N-diethylacetamide (14). White solid. Mp 142-143 °C. ^{1}H NMR (300 MHz, DMSO) δ 7.87-7.81 (m, 4H), 6.90 (s, 1H), 3.89 (s, 2H), 3.50 (q, *J* = 7.2 Hz, 2H), 3.31 (s, 3H), 3.24 (q, *J* = 7.1 Hz, 2H), 2.69 (s, 3H), 2.34 (s, 2H), 1.93 (d, *J* = 13.8 Hz, 4H), 1.79 (s, 2H), 1.65 (d, *J* = 11.0 Hz, 6H), 1.19-1.13 (m, 3H), 0.9 (t, *J* = 7.2 Hz, 3H); ^{13}C NMR (75 MHz, DMSO) δ 169.2, 163.0, 158.4, 152.5, 147.6, 145.2, 136.4, 132.9, 130.5, 116.3, 109.5, 105.5, 102.2, 58.0, 42.1, 37.0. 35.3, 33.7, 27.7, 26.4, 24.7, 16.7, 14.7, 13.5; HRMS (m/z): $[M+Na]^+$ calculated for 719.1706, found 719.1703.

3. NMR Spectra

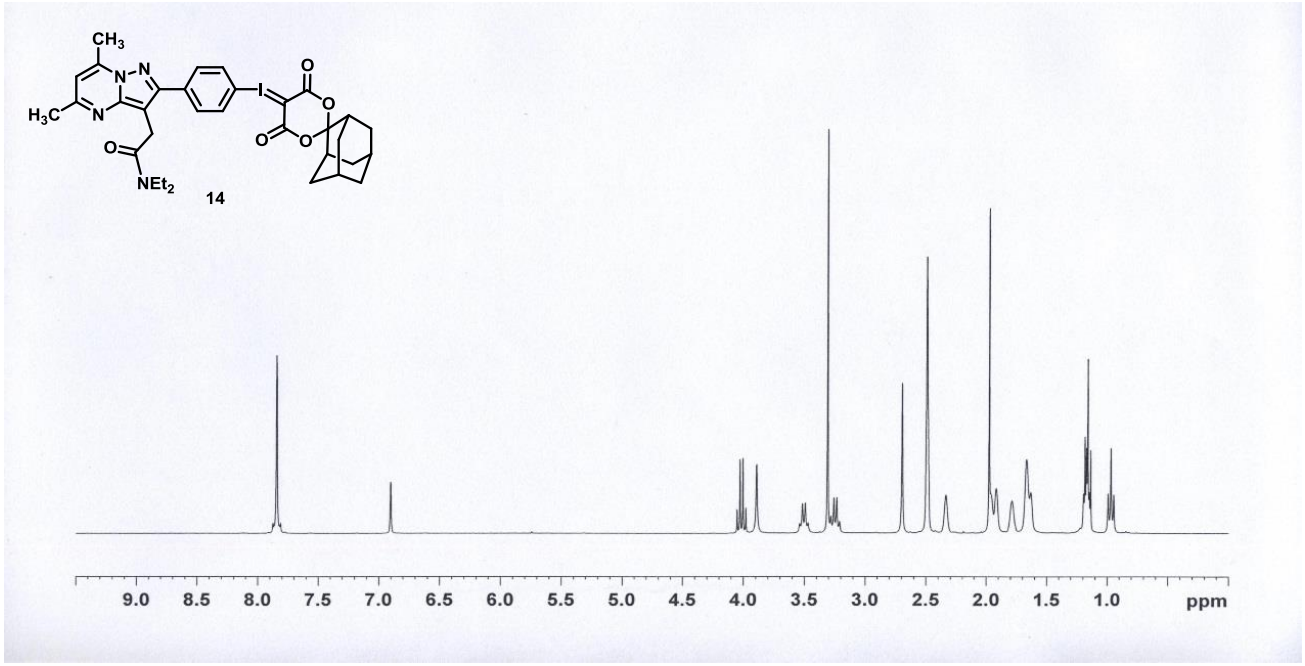

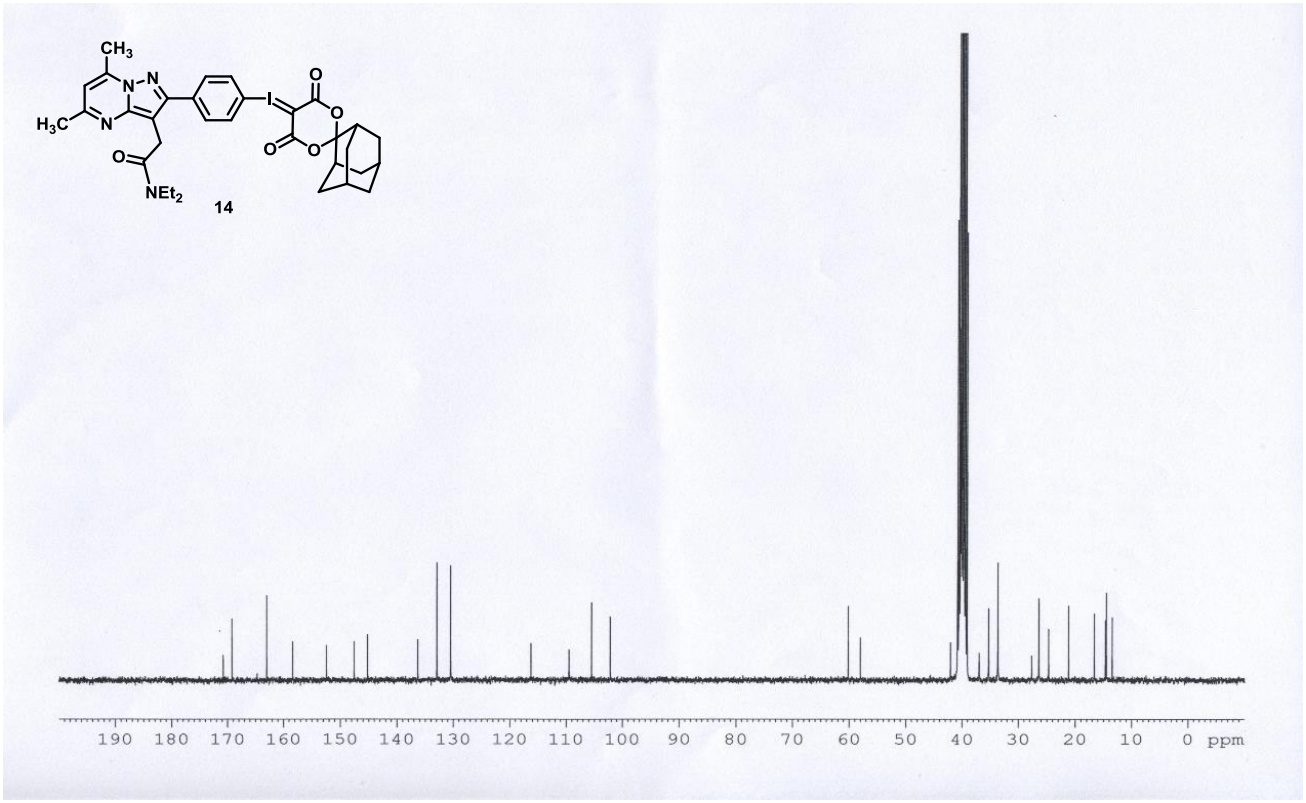

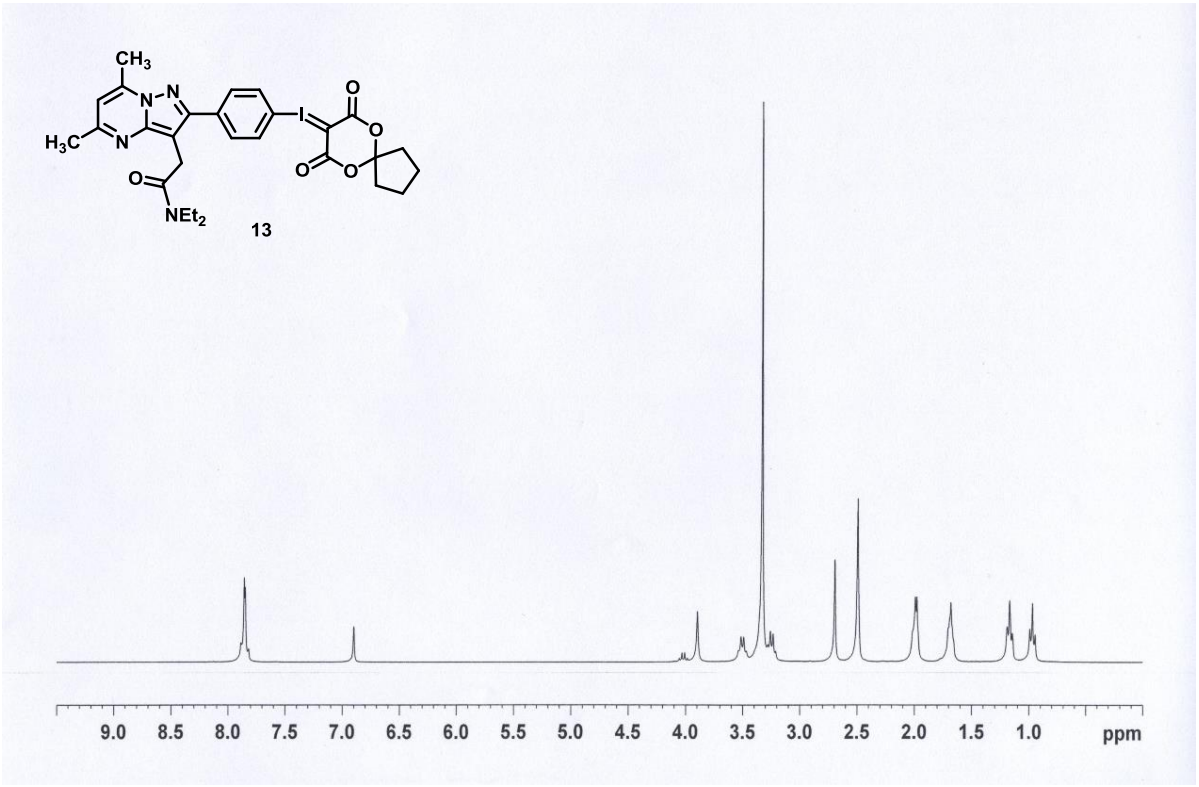
CH3
H3C
N
N
N
I
O
O
O
O
O
NEt2
13
9.0
8.5
8.0
7.5
7.0
6.5
6.0
5.5
5.0
4.5
4.0
3.5
3.0
2.5
2.0
1.5
1.0
ppm

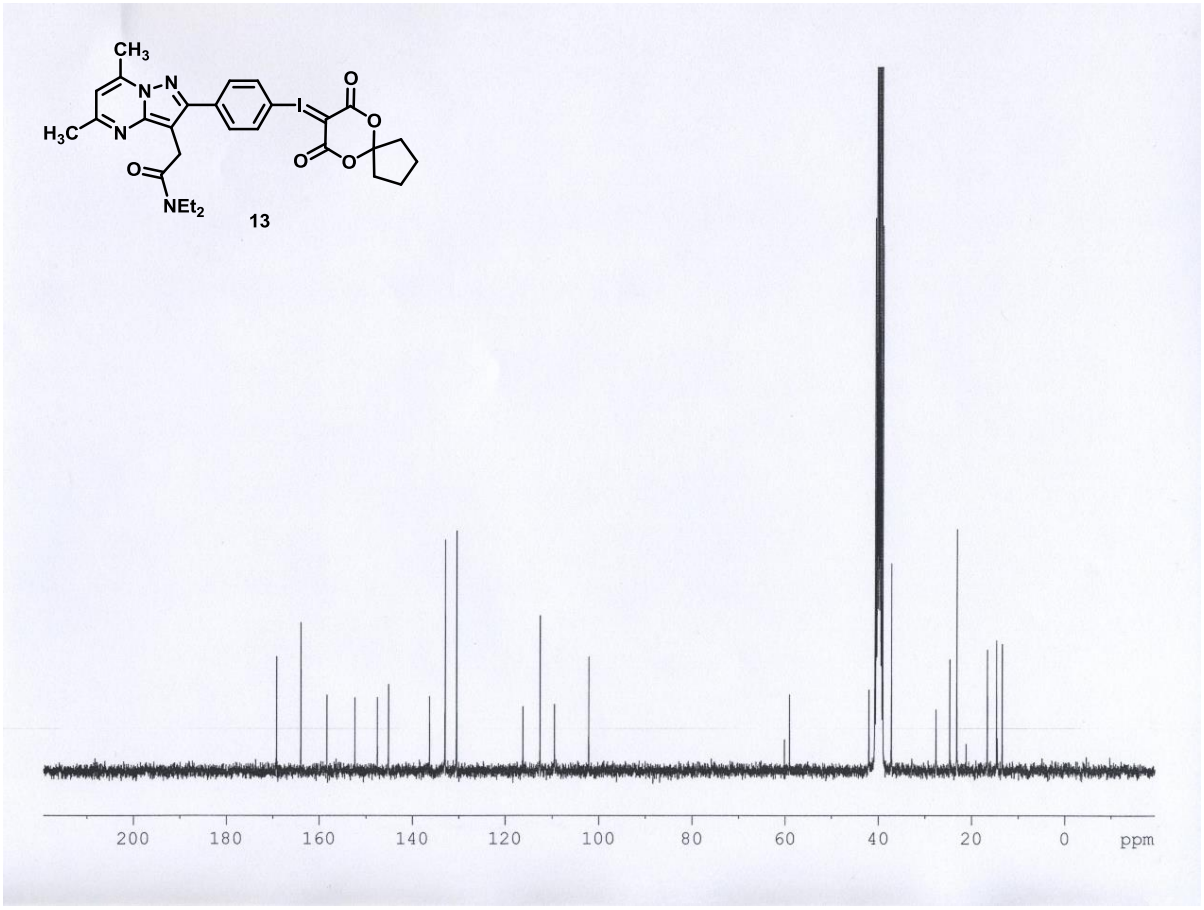
CH3
H3C
N
N
N
I
O
O
O
O
O
NEt2
13
200
180
160
140
120
100
80
60
40
20
0
ppm

4. *In vitro* binding assays

The affinity of **10** (FDPA) for the TSPO was evaluated with the assistance of National Institute of Mental Health's Psychoactive Drug Screening Program (NIMH PDSP),[3] using of a membrane-binding assay with[^{3}H]PK11195 as the radioligand and rat kidney tissue.[4]

A solution of **10** is prepared as a 1.0 mg/ml stock in the appropriate 50 mM Tris buffer. A similar stock of Ro5-4864 is also prepared. Eleven dilutions (5 x assay concentration) of **10** and Ro5-4864 are prepared in the appropriate 50 mM Tris buffer by serial dilution: 0.05 nM, 0.5 nM, 1.5 nM, 5 nM, 15 nM, 50 nM, 150 nM, 500 nM, 1.5 μM, 5 μM, 50 μM (thus, the corresponding assay concentrations span from 10 pM to 10 μM and include semilog points in the range where high-to-moderate affinity ligands compete with radioligand [^{3}H]PK11195 for binding sites).

[^{3}H]PK11195 is diluted to five times the assay concentration in 50 mM Tris-acetate, pH 7.4. Typically, the assay concentration of [^{3}H]PK11195 is a value between one half the K_D and the K_D of a particular radioligand at its target.

Aliquots (50 μl) of [^{3}H]PK11195 are dispensed into the wells of a 96-well plate containing 100 μl of 50 mM Tris-acetate, pH 7.4. Then, duplicate 50-μl aliquots of **10** and Ro5-4864 dilutions are added.

Finally, crude membrane fractions prepared from rat brain homogenate for TSPO PK11195 site, from transfected cells in 10 cm plates (by harvesting PBS-rinsed monolayers, re-suspending and lysing in chilled, hypotonic 50 mM Tris-acetate, pH 7.4, centrifuging at 20,000 x g, decanting the supernatant and storing at -80 degrees centigrade; typically, one 10 cm plate provides sufficient material for 24 wells) are re-suspended in 3 ml of chilled 50 mM Tris-acetate, pH 7.4 and homogenized by several passages through a 26 guage needle, then 50 μl are dispensed into each well.

The 250 μl reactions are incubated at room temperature and shielded from light for 1.5 hours, then harvested by rapid filtration onto Whatman GF/B glass fiber filters pre-soaked with 0.3% polyethyleneimine using a 96-well Brandel harverster. Four rapid 500 μl washes are performed with chilled 50 mM Tris-acetate to reduce non-specific binding. Filters are placed in 6 ml scintillation tubes and allowed to dry overnight. The next day, 4 ml of EcoScint scintillation cocktail (National Diagnostics) are added to each tube. The tubes are capped, labeled, and counted by liquid scintillation counting.

Raw data (dpm) representing total [^{3}H]PK11195 binding (i.e., specific + nonspecific binding) are plotted as a function of the logarithm of the molar concentration of the competitor (i.e., **10** or Ro5-4864). Non-linear regression of the normalized raw data is performed inPrism 4.0 (GraphPad Software)

using the built-in three parameter logistic model describing ligand competition binding to [^{3}H]PK11195-labeled sites:

$$y = \text{bottom} + [(\text{top-bottom})/(1 + 10^{x\text{-log}IC50})]$$

where bottom equals the residual [^{3}H]PK11195 binding measured in the presence of 10 μM Ro5-4864 (i.e., non-specific binding) and top equals the total[^{3}H]PK11195 binding observed in the absence of competitor. The logIC_{50} is thus estimated from the data and used to obtain the K_i by applying the Cheng-Prusoff approximation:

$$K_i = IC_{50}/(1 + [\text{ligand}]/K_D)$$

where [ligand] equals [^{3}H]PK11195 concentration and K_D equals the affinity constant of [^{3}H]PK11195 for TSPO receptor.

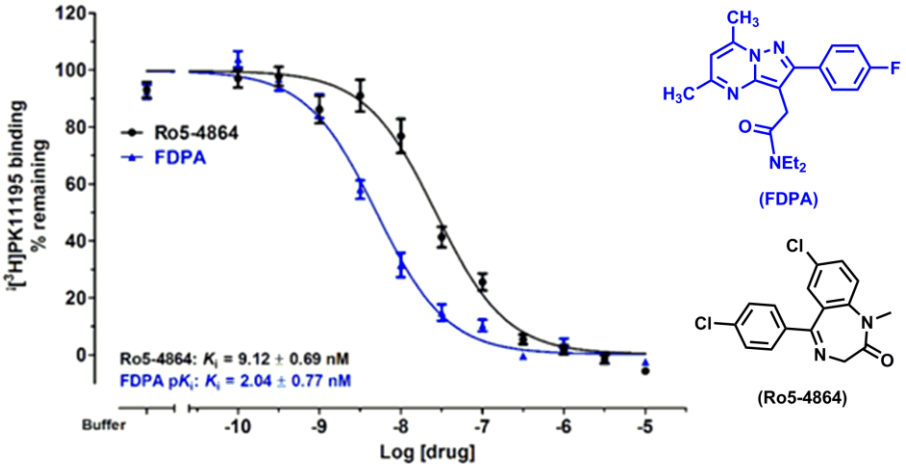

Figure S1. *In vitro* binding affinity of FDPA for TSPO.

5. Radiofluorination of [^{18}F]2

(1) Stability of ylide precursor 14 monitored by ^{1}H NMR

The thermostability of ylide precursor **14** was perfect since no decomposition was detected by ^{1}H NMR after heating at 120 ºC for 10 min (Figure S2 A & B). However, when 1 mg of TEAB was added, **14** was decomposed quickly, even without heating (Figure S2 C & D).

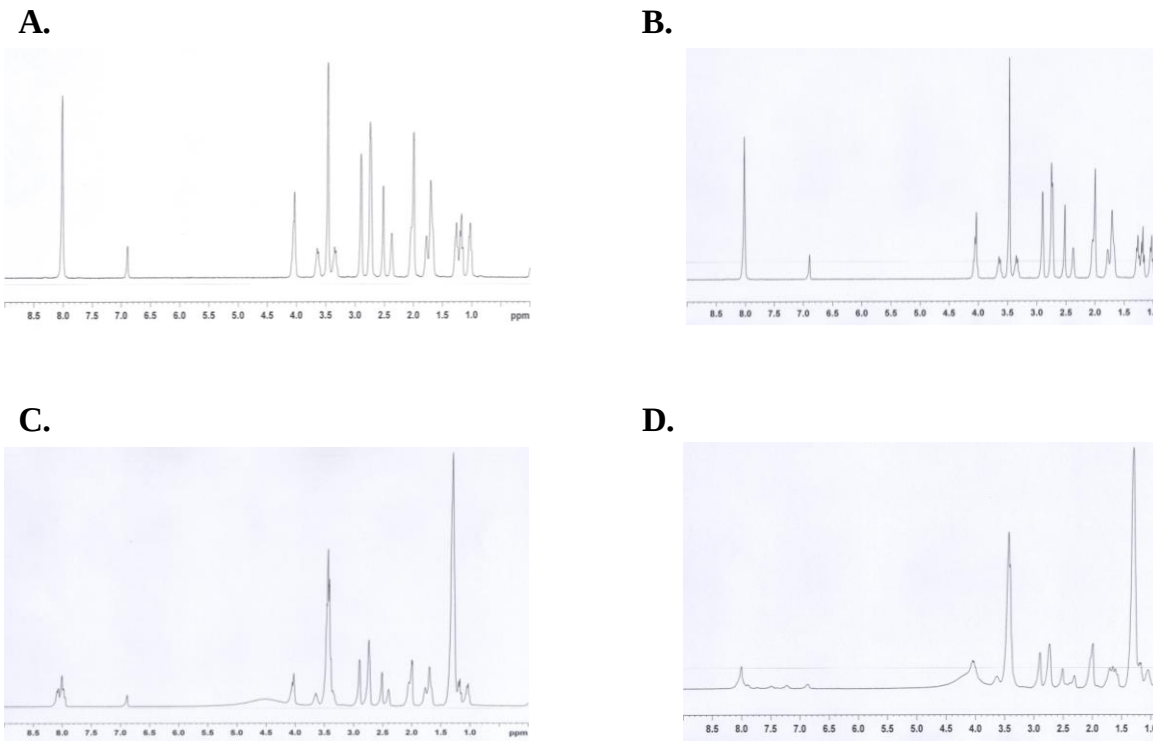

Figure S2. Stability of Ylide Precursor **14** in Basic Conditions. A) Ylide **14** in d_7-DMF (t = 0, T = room temperature). B) Ylide **14** in d_7-DMF (120 ºC for 10 min). C) Ylide **14** + 1 mg of TEAB in d_7-DMF (t = 0, T = room temperature). D) Ylide **14** + 1 mg of TEAB in d_7-DMF (120 ºC for 3 min).

(2) Optimization Conditions

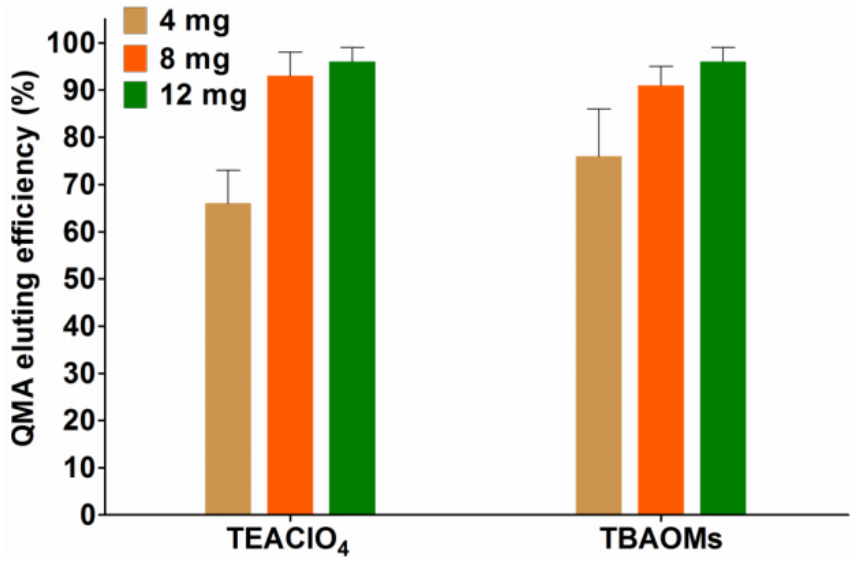

Figure S3. QMA eluting efficiency test (n = 3). 12 mg of TBAOMs or $TEAOCl_4$ as eluting salts could give more than 95% $[^{18}F]F^-$ eluting efficiency from Waters Sep-Pak Light QMA.

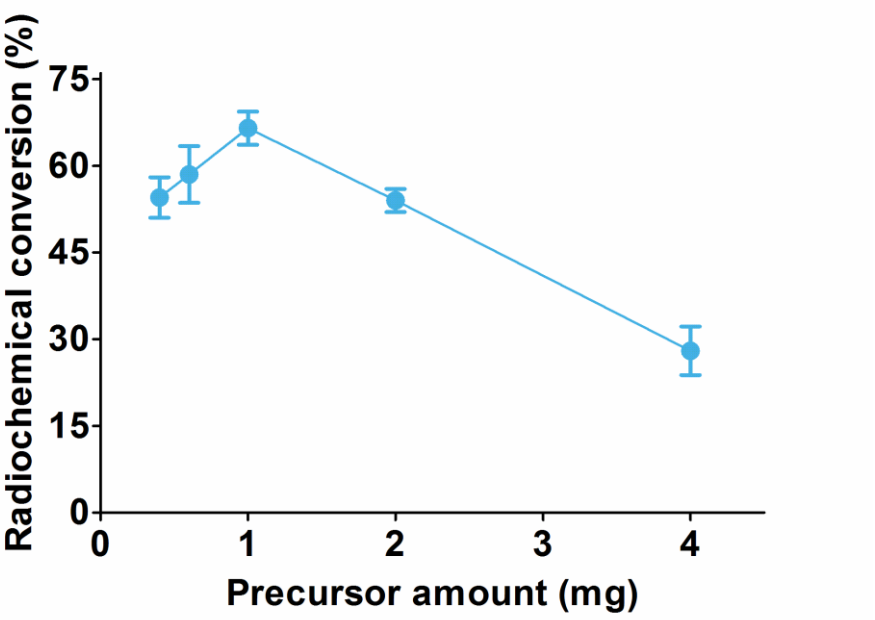

Figure S4. Precursor loading effect (n = 3). Conditions: Precursor **14**, TBAOMs (12 mg), CH_3CN (1.0 mL), 120 ºC, 15 min.

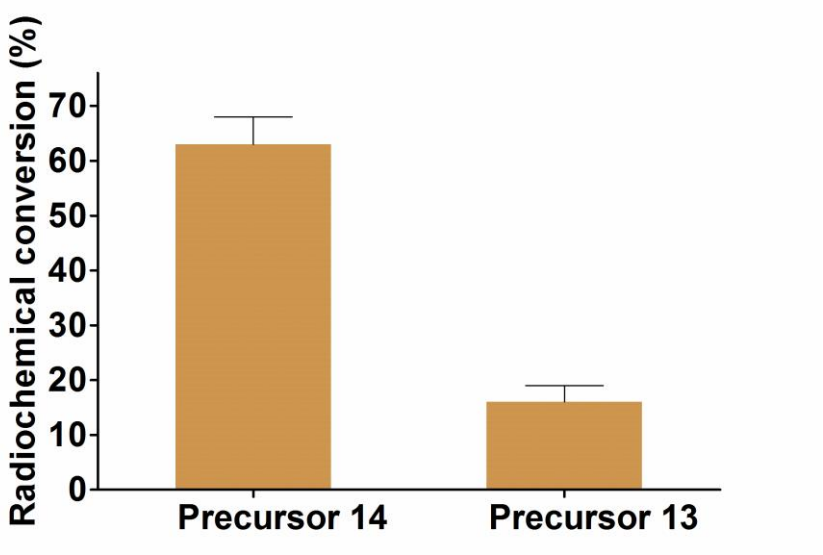

Figure S5. Precursor type effect (n = 3). Conditions: Precursors **14** or **13** (2 mg), TBAOMs (12 mg), CH_3CN (1.0 mL), 120 ºC, 15 min.

Quality control with co-injection of **10** (FDPA) as a reference

Column: Phenomenex Luna C18, 250 x 4.6 mm, 5 µm

Mobile phase: 70% MeCN, 30% 0.1 M NH_4•HCO_2(aq)

Flow rate: 1 mL/min

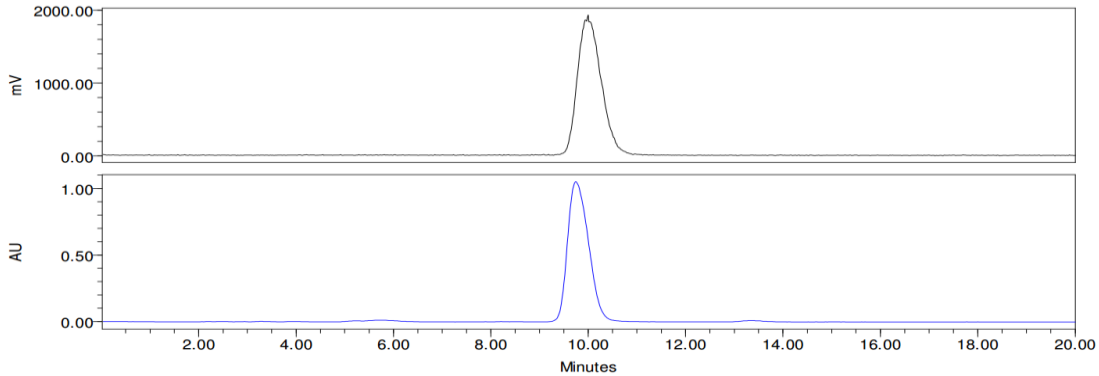

Figure S6. HPLC spectra of isolated product with co-injection of **10**.

6. *In vitro* stability in normal mouse serum

The freshly prepared ethanol solution of **[^{18}F]2** (10 μL) was mixed with aliquots of normal mouse serum (100 μL; x 5; Abcam Inc., MA, USA) and incubated with agitation (550 rpm) at 37 °C. At 20, 40, 60, 90, 120 min, these aliquots (40 μL) were mixed with an equal volume of CH_3CN, stirred in a vortex mixer, followed by centrifuge (6,000 rpm for 2 min) to precipitate serum proteins. A portion of the supernatant was subjected to radioHPLC analysis using an on-line radioactivity detector.

7. Measurement of lipophilicity ("the shake flask method")

The measurement of Log*D* value was commenced by mixing **[^{18}F]2** (radiochemical purity ~100%) with *n*-octanol (3.0 g) and sodium phosphate buffer (PBS; 3.0 g, 0.1 M, pH 7.4) in a test tube. The tube was vortexed for 3 min at room temperature, followed by centrifuge (~3500-4000 rpm) for additional 5 min. An aliquot of PBS and *n*-octanol (0.50 mL each) was removed, weighted and the radioactivity in each component was measured using a 2480 Wizard automatic gamma counter (Perkin Elmer, Inc.) The Log*D* value was determined by Log [ratio of radioactivity between the *n*-octanol and PBS solutions] (n = 5).

8. *Ex vivo* biodistribution data

tissue	2 min	25 min	45 min
blood	4.06 ± 1.3	0.48 ± 0.15	0.22 ± 0.03
brain	3.69 ± 0.18	1.59 ± 0.27	1.15 ± 0.46
lungs	9.55 ± 3.23	11.23 ± 1.27	6.34 ± 1.87
heart	25.66 ± 4.24	9.69 ± 1.36	8.71 ± 1.78
liver	9.13 ± 5.07	7.98 ± 0.40	8.97 ± 4.77
kidney	14.79 ± 4.16	20.63 ± 6.23	29.07 ± 0.93
spleen	3.56 ± 0.01	6.20 ± 2.35	9.98 ± 0.95
pancreas	12.92 ± 1.84	5.63 ± 1.01	5.24 ± 2.09
small intestine	5.00 ± 0.05	4.68 ± 1.19	5.96 ± 1.11
muscle	0.62 ± 0.29	0.73 ± 0.18	0.64 ± 0.14
bone	0.51 ± 0.17	0.55 ± 0.14	0.52 ± 0.12
adrenal	28.71 ± 1.59	31.28 ± 4.47	38.00 ± 1.52

Table S1. *Ex vivo* biodistribution of **[^{18}F]2** in mice. Date are expressed as %ID/g (mean ± SD, n = 3)

tissue	2 min	25 min	45 min
blood	0.65 ± 0.21	0.08 ± 0.03	0.04 ± 0.00
brain	0.59 ± 0.03	0.26 ± 0.03	0.20 ± 0.08
lungs	1.53 ± 0.52	1.86 ± 0.29	1.08 ± 0.32
heart	4.10 ± 0.68	1.59 ± 0.16	1.48 ± 0.30
liver	1.46 ± 0.81	1.43 ± 0.15	1.52 ± 0.81
kidney	2.37 ± 0.67	3.43 ± 1.17	4.94 ± 0.16
spleen	0.57 ± 0.01	1.03 ± 0.43	1.70 ± 0.16
pancreas	2.07 ± 0.29	0.92 ± 0.13	0.89 ± 0.36
small intestine	0.80 ± 0.01	0.78 ± 0.23	1.01 ± 0.19
muscle	0.10 ± 0.05	0.12 ± 0.03	0.11 ± 0.02
bone	0.08 ± 0.03	0.09 ± 0.02	0.08 ± 0.02
adrenal	4.59 ± 0.26	5.18 ± 0.96	6.46 ± 0.26

Table S2. *Ex vivo* biodistribution of **[^{18}F]2** in mice. Date are expressed as SUV. (mean ± SD, n = 3)

9. Whole body PET images of wide type mice for validating bone uptake

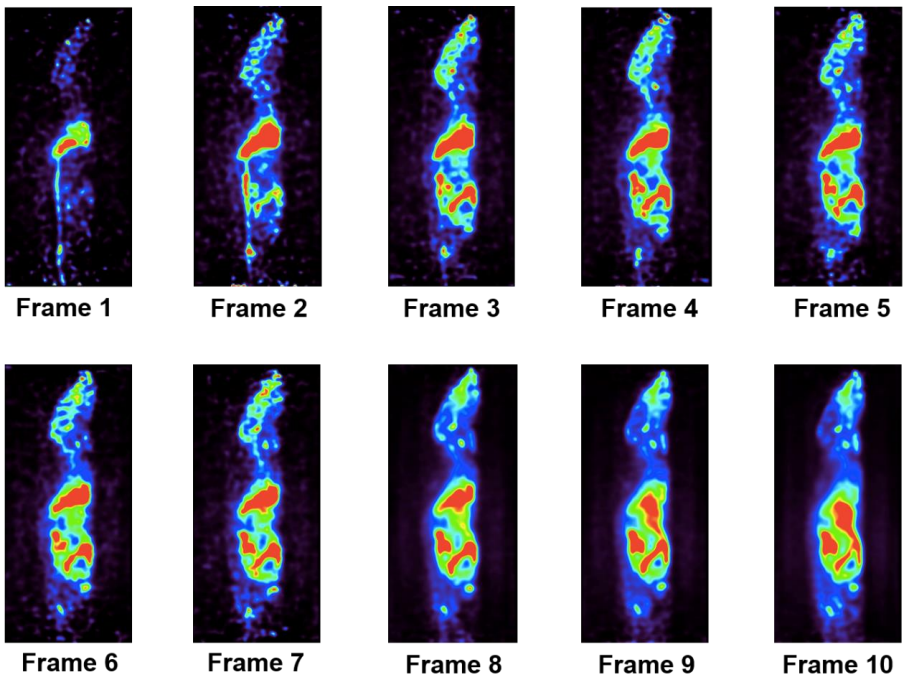

Figure S7. Representative whole body PET images of wide type mice. Sofie G4 microPET scanner, frames× min: 2 × 0.5, 5 × 1, 2 × 12, 1 × 30

Note: Little or neglectable bone uptake was observed during the scanning period, confirming no significant radiodefluorination of **[^{18}F]2** *in vivo*.

10. Mouse models

Ischemic models. Justification for ischemia models: In the healthy brain, TSPO expression is low and can be found in astrocytes, microglia, endothelial, cells using antibody stainings. (*Neuropathol Appl Neurobiol.* **2009**, *35,* 306–328) After ischemic injury, TSPO level is increased in microglia within the first days after the insult. (*Prog Neurobiol.* 2006, **80**, 308–322; *Pharmacol Ther.* 2008, **118**, 1–17*; J Cereb Blood Flow Metab.* 2010, **30**, 230–241.) This observation makes TSPO a potential marker to detect early inflammatory changes throughout the injured brain.

Mild focal ischemia was produced by intraluminal occlusion of the middle cerebral artery for 30 min using an intraluminal thread model, as mentioned in our previous work.[5-7] In general, Sprague–Dawley rats were anesthetized with 4% (v/v) isoflurane and maintained under anesthesia with 1.8% isoflurane. A 2.0-monofilament nylon suture coated with silicon was inserted into the internal carotid artery up to the level of the middle cerebral artery branches (approximately 20 mm from the internal carotid artery), and the neck incision was closed with a silk suture. Thirty min after regaining consciousness from anesthesia, rats were again anesthetized and the filament was carefully removed for reperfusion. Body temperature was monitored and maintained at optimal levels throughout the surgery. The rats were then used for PET imaging or metabolite analysis at 7 days post ischemic surgery.

Transgenic mouse model of Alzheimer's disease (APP/PS1). Justification for AD models: Neuroinflammation occurs at the pre-plaque stage and serves as a major driving force of Alzheimer's disease. (*Lancet Neurol*, **2015**, *14*, 388-405; *Trends Neurosci* **2015**, *38*, 621-636.) It has been reported that TSPO expression is significantly increased in the activated microglial cells during brain inflammation in AD (*Brain Res*, **1987**, *421*, 167-172). In a recent paper, Liu *et al.* used double and triple immunofluorescence staining to assess the colocalization between TSPO and Aβ, microglia, and astrocytes (*J Neurosci*, **2015**, *35*, 15716-15730). The results confirmed that TSPO was mainly expressed in activated microglia and co-localized with Aβ of APP/PS1dE9 transgenic mouse brain (the same animal model that we used in this work). The association of Aβ deposition and TSPO-positive microglia was also observed in human AD brain sections.

Strain B6C3-Tg (APPswe, PSEN1dE9) 85Dbo/J Female; purchase from the Jackson Laboratory. 12-month old when they were imaged.

11. PET imaging studies

Ischemic rat models. PET scans were conducted using a small-animal PET scanner (Inveon; Siemens Medical Solutions, Knoxville, TN, USA). For the ischemic brain imaging studies, 7 days after ischemic surgery, a rat was anesthetized with 1–2% isoflurane during the scan and its body temperature was maintained with a 37 °C water circulation system (T/Pump TP401, Gaymar Industries, Orchard Park, NY, USA). An emission scan was immediately acquired for 90 min after injection of **[^{18}F]2** (16-21 MBq; 432-567 μCi) / 0.1-0.2mL) through the tail vein. For the displacement experiments, unlabeled PK11195 (3 mg/kg in 1 mL of saline containing 10% ethanol and 5% Tween 80) was injected 1 min after the injection of **[^{18}F]2**. Each experiment was performed in a group of three animals. PET data modeling was performed into three-dimensional sinograms, which were changed into two-dimensional sonograms (frames × min: 4 × 1, 8 × 2, 14 × 5) by Fourier rebinning. Filtered back-projection using Hanning's filter with a Nyquist cut-off frequency of 0.5 cycle/pixel was used for dynamic image reconstruction. PET images were analyzed using ASIPro VM^{TM} (Analysis Tools and System Setup/Diagnostics Tool; Siemens Medical Solutions) with reference to the magnetic resonance (MR) imaging template. A region of interest (ROI) with fixed size was manually positioned at the center of the striatum on the ipsilateral side defined on a summation image for each experiment, which coincided to the ROI used in autoradiography. The ipsilateral ROI was copied and symmetrically pasted into the contralateral striatum on the same slice to yield a contralateral ROI of identical volume and shape. Time activity curves (TACs) for ipsilateral and contralateral striatum were generated. Decay correction was performed for the brain uptake of radioactivity with reference to the injection time and expressed as the standardized uptake value (SUV), which was normalized for the injected radioactivity and body weight. The SUV was calculated according to the following formula: SUV = (radioactivity per cubic centimetre tissue/injected radioactivity) × grams body weight.

The binding potential (BP_{ND}) was calculated as a quantitative value, which represented the receptor binding with the radioligand, using PMOD software (PMOD Technologies, Zurich, Switzerland). The BP_{ND} was estimated using a simplified reference-tissue model (SRTM) by taking the TAC of the contralateral side as the reference region instead of the plasma input function. The SRTM analysis in the ipsilateral side of the striatum and cerebral cortex was performed using the TAC in the contralateral side as a reference region.[8]

APP/PS1 transgenic mouse models. [^{18}F]2 (1.67 MBq; 45 μCi) was injected into the tail-vein of each animal. Mice were serially imaged dynamically using a Sofie G4 microPET (frames× min: 2 × 0.5, 5 × 1, 2 × 12, 1 × 30). For all imaging experiments, mice were anesthetized using 2% isoflurane in O_2 at a flow rate of ~1.5 L/min, positioned in a prone position along the long axis of the microPET

scanner and imaged. Images were reconstructed using a filtered back projection reconstruction algorithm. For image analysis, regions of interest (ROIs) were manually drawn from three-dimensional filtered back projection (FBP) reconstructed PET images using AMIDE software. Regional radioactivity was expressed as the percentage standardized uptake value [% SUV = % ID/mL × body weight (g)]. Two- and three-dimensional visualizations were produced using the DICOM viewer OsiriX (© Pixmeo SARL, 2003-2014).

12. *In vitro* autoradiography

Ischemia. Brain coronal sections (20 μm) were prepared from frozen rat brains using a cryostat (HM560, Carl Zeiss, Oberkochen, Germany). The brain sections were pre-incubated for 20 min in 50 mM Tris-HCl buffer (pH 7.4) at 25 ºC followed by incubation in the same buffer containing **[^{18}F]2** (1.85 MBq (50 μCi) / 200 mL) at 25 ºC for 60 min. For the inhibition studies, unlabeled PK11195 (10 μM, prepared from 2 mM PK11195 solution in Tris containing 10% ethanol and 5% Tween 80) was co-incubated with **[^{18}F]2**. After incubation, the brain sections were washed with Tris 5 min x 2, DW 10 sec x 1. Autoradiograms were acquired using a Bio-Imaging analyzer system (BAS-5000, Fujifilm, Tokyo, Japan). The radioactivity level on the brain regions was measured by the Multi Gauge analysis software version 2.3 (Fujifilm) and expressed as photo-stimulated luminescence per unit area (PSL/mm^2).

Alzheimer's disease. Brain slices from APP/PS1 mice and age-matched controls were washed with double-distilled water for 5 min, and then fixed with 4% formalin for 5 min, and washed with double-distilled water. The slices were subsequently dried, then incubated with 0.2 MBq (5 μCi) of **[^{18}F]2** for 30 min. The slices were then washed with 20% ethanol double-distilled water and dried. The dried slices were exposed to an imaging plate for 1 hour, and the plate was scanned with autoradiography system Cyclone (Perkin Elmer).

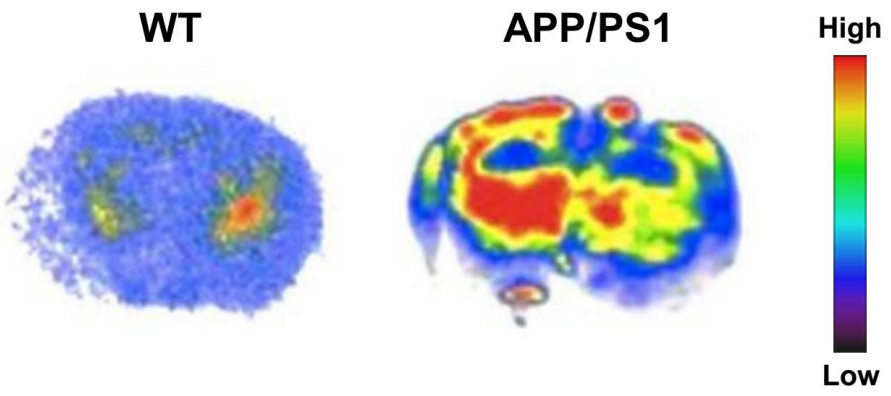

Figure S8. *In vitro* autoradiography of **[^{18}F]2** in wild type and APP/PS1 mouse brains

****

References

1. Selleri, S.; Bruni, F.; Costagli C.; et al. 2-Arylpyrazolo[1,5-a]pyrimidin-3-yl Acetamides. New Potent and Selective Peripheral Benzodiazepine Receptor Ligands. *Bioorg. Med. Chem.* **2001**, *9*, 2661-2671.

2. Damont, A.; Medran-Navarreté, V.; Cacheux F.; et al. Novel Pyrazolo[1,5-a]pyrimidines as Translocator Protein 18 kDa (TSPO) Ligands: Synthesis, *in Vitro* Biological Evaluation, [^{18}F]-Labeling, and *in Vivo* Neuroinflammation PET Images. *J. Med. Chem.* **2015**, *58*, 7449-7464.

3. NIMH PDSP. http://pdspdb.unc.edu/pdspWeb/.

4. Nadler, L. S.; Raetzman, L. T.; Dunkle, K. L.; et al. GABAA receptor subunit expression and assembly in cultured rat cerebellar granule neurons. *Brain Res. Dev. Brain Res.* **1996**, *97*, 216-225.

5. Tiwari, A. K.; Ji, B.; Yui, J.; et al. [^{18}F]FEBMP: Positron Emission Tomography Imaging of TSPO in a Model of Neuroinflammation in Rats, and *in vitro* Autoradiograms of the Human Brain. *Theranostics* **2015**, *5*, 961-969.

6. Tiwari, A. K.; Yui, J.; Fujinaga, M.; et al. Characterization of a novel acetamidobenzoxazolone-based PET ligand for translocator protein (18 kDa) imaging of neuroinflammation in the brain. *J. Neurochem.* **2014**, *129*, 712-720.

7. Yui, J.; Hatori, A.; Kawamura, K.; et al. Visualization of early infarction in rat brain after ischemia using a translocator protein (18 kDa) PET ligand [^{11}C]DAC with ultra-high specific activity. *Neuroimage* **2011**, *54*, 123-130.

8. Lammertsma, A. A.; Hume, S. P. Simplified reference tissue model for PET receptor studies. *Neuroimage* **1996**, *4*, 153-158.